Nonlinear Dyn (2015) 80:1063–1079
DOI 10.1007/s11071-014-1556-1

ORIGINAL PAPER

Power flow behaviour and dynamic performance of a nonlinear vibration absorber coupled to a nonlinear oscillator

J. Yang · Y. P. Xiong · J. T. Xing

Received: 2 January 2014 / Accepted: 21 June 2014 / Published online: 11 July 2014

Abstract The vibrational power flow characteristics of a two-degree-of-freedom system are investigated to examine the performance of nonlinear absorbers in vibration attenuation of nonlinear primary oscillators. The nonlinearities in the oscillator and those in the absorber are both characterised by cubic restoring and damping forces. Both analytical approximations and numerical integrations are used to obtain time-averaged power flow variables, as well as kinetic energies of the system. Power absorption ratio and the kinetic energy of the nonlinear oscillator are proposed to quantitatively evaluate the effectiveness of nonlinear absorbers with respect to the existing nonlinearities in the oscillator. Comparing with linear absorbers, it is found that softening (hardening) stiffness absorber provides benefits for vibration mitigation of a hardening (softening) stiffness primary oscillator by enhancing power absorption efficiency and reducing the kinetic energy of the oscillator so that the functioning frequency range of the absorber can be enlarged. Nonlinear cubic damping in the absorber is shown beneficial for vibration suppression as the power absorption ratio becomes large at resonance frequencies so that the peak power flow and kinetic energy levels are reduced. The developed model can be conveniently extended to study other types of nonlinearities in the absorber/oscillator. Conclusions and suggestions are provided for applications.

Keywords Power flow analysis · Nonlinear vibration absorber · Nonlinear oscillator · Nonlinear stiffness · Nonlinear damping

J. Yang · Y. P. Xiong (✉) · J. T. Xing
Fluid Structure Interactions Research Group, Faculty of Engineering and the Environment, University of Southampton, Boldrewood Campus, SO16 7QF Southampton, UK
e-mail: y.xiong@soton.ac.uk

1 Introduction

Linear dynamic vibration absorbers (DVAs) are widely used for suppressing excessive vibrations of linear primary structures. The design concept was originally reported about a century ago by Frahm [1] who added an undamped linear attachment to a conservative linear oscillator to suppress its vibrations. Mathematical treatments were later provided to a vibration absorption system with consideration of weak damping in the absorber as an energy dissipation mechanism [2,3]. It was shown that if the natural frequency of the absorber was tuned to that of the linear oscillator, effective attenuations of its vibrations can be achieved, when the excitation frequency is the same as the natural frequency. Since then, different optimisation criteria have been proposed for optimal designs of absorbers by varying the stiffness and/or damping parameters. For instance, the classical approach by Omondroyd and Den Hartog [2] optimised the damping ratio of the absorber so that the two peak values in the displacement response curves of the coupled system were the same and the derivatives at the peaks vanished. On the other hand, much

research has also been undertaken on the applications of linear absorbers to passive vibration control of more complicated linear systems. For example, Snowdon [4] attached DVAs to simply supported plate structures to suppress their vibrations and investigated optimum conditions of tuning and damping. Ozer and Royston [5] extended Den Hartog's design approach of invariant points to determine optimal damping of vibration absorbers for undamped multiple degree-of-freedom (DOF) systems. However, one deficiency often confining the applications of linear vibration absorbers is that they are only effective in a relatively narrow band of excitation frequencies.

To broaden the working frequency range of linear vibration absorbers, the feasibility of employing nonlinear absorbers for linear dynamical systems has been explored. Early studies of these were conducted by Roberson [6], Pipes [7] and Arnold [8], who considered undamped nonlinear absorbers with stiffness nonlinearities and suggested that softening stiffness would be beneficial in vibration suppression. Hunt and Nissen [9] proposed practical softening-type absorbers with linear viscous damping and showed that they can be used to double the frequency bandwidth for effective vibration absorption. Rice [10] examined the stabilities of a nonlinear stiffness absorber and showed a possible existence of unstable periodic solutions near the tuning frequency. Jordanov and Cheshankov [11] proposed an efficient numerical method for minimisation of the vibration response to obtain the optimal parameters for both linear and nonlinear dynamic vibration absorbers.

It should be noted that many dynamical systems encountered in engineering practice are inherently nonlinear and significant nonlinearity has been observed in many applications. For example, intrinsic nonlinearities in suspensions bridges can lead to large-amplitude periodic oscillation, as well as significant travelling waves [12]. The mounts for hydraulic engine used in automobiles possess nonlinearity in both damping and stiffness [13]. As such systems can exhibit complex nonlinear phenomena such as modal interaction, bifurcation, chaos, successful application of DVAs to reduce their vibrations is still challenging task and has attracted increasing attention of many researchers. Natsiavas [14] examined the steady-state responses of a system with a nonlinear absorber as well as a nonlinear primary structure and showed that stiffness nonlinearity can assist vibration absorption by suppressing response peaks. Bosnel et al. [15] showed experimentally that a linear dynamical absorber may be used to suppress primary or super/sub- harmonic resonances of a piece-wise linear beam. Jo and Yabuno [16] devised a pendulum absorber for vibration absorption of a main system subjected to a nonlinear restoring force and experimentally verified its efficiency. Based on the frequency energy dependence characteristics of nonlinear systems, Viguié and Kerschen [17] proposed a qualitative tuning approach of nonlinear dynamic absorbers to reduce the impulsive response of nonlinear oscillators. Ji and Zhang [18] used a linear absorber to reduce the primary resonance vibrations as well as to eliminate saddle-node bifurcation and jump phenomenon of a nonlinear structure. Using the saturation phenomenon, Oueini et al. [19] designed and analysed a nonlinear active vibration absorber for flexible structures with quadratic nonlinearities and showed that the absorber was effective, when the primary structure was excited near its resonances. Febbo and Machado [20] investigated the performance of a nonlinear absorber with a finite extensibility nonlinear elastic potential and showed that vibration absorption can be achieved over a large excitation frequency range.

In previous investigations of nonlinear DVAs, however, the displacement response of the primary structure was often used to assess vibration absorption performance. The associated vibrational power flow behaviour of the system is usually ignored. The vibrational power flow analysis approach provides a valuable tool to characterise the dynamic behaviour of complex systems, incorporating the effects of force and velocity, as well as their relative phase angle in a single quantity [21]. It has been developed to study linear passive/active vibration control systems [22–27]. Recently, Zilletti et al. [28] used the kinetic energy of the primary system and the time-averaged absorbed power as optimisation objectives of a linear dynamic absorber attached to a linear oscillator.

There is also a growing interest in vibrational power flow behaviour of nonlinear dynamical systems. For example, Royston and Singh [29] examined the energy flow in a hydraulic engine mount system and showed that significant amount of vibration energy can be transmitted through a nonlinear path to a flexible base. Xing and Price [30] provided a generalised mathematical model based on a substructure method to analyse the power flows in linear continuous systems connected

by nonlinear springs and dampers. Xiong et al. [31] examined an integrated system of a machine, a nonlinear isolator and a flexible beam-like ship excited by sea waves. The results showed that the time-averaged power flow spectra were significantly affected by the isolator nonlinearities when the excitation frequency was close to resonant frequencies. Vakakis et al. [32] discovered the phenomenon of targeted energy transfer, based on which nonlinear attachment can be used to channel and dissipate the vibration energy of a main structure. Xiong and Cao [33] investigated the power flow characteristics of a two-degrees-of-freedom system with a nonlinear stiffness absorber and a linear primary structure. Yang et al. [34,35] developed power flow analysis (PFA) approaches for nonlinear dynamical systems, re-examined typical nonlinear systems from the power flow perspective, and demonstrated the applications of PFA to vibration control and vibration energy harvesting systems. It was found that as the averaging time increases, the time-averaged power flow of a chaotic response tends to an asymptotic value insensitive to the initial conditions [36]. Therefore, it provides an indicator to quantify both periodic and chaotic responses, and allows comparisons of the associated vibration levels.

For better designs and applications of nonlinear dynamic absorbers, a comprehensive study of the power flow characteristics of a nonlinear vibration absorption system is necessary. In particular, the performance of nonlinear absorbers is of interest when different types of damping and stiffness nonlinearities exist in the primary oscillator. In this paper, we seek to address the issue by analytical and numerical methods to reveal vibration power input, transmission, dissipation and absorption in such a system. The influences of different combinations of damping/stiffness nonlinearities in a vibrating oscillator and in the absorber on the power flow behaviour of the integrated system will be examined. Cubic restoring and damping forces are considered in the oscillator and the absorber. The former is a typical model for nonlinear stiffness, with the same form as the well-known Duffing oscillator. The latter has been used to account for nonlinear viscous damping effects. However, the analysis methodology developed in the paper can be easily extended to other types of nonlinearities represented by polynomial or trigonometric functions. Following a description of the mathematical model of the system, the solution procedures for power flows quantities are outlined. The method of averaging is used to obtain analytical approximations of system responses and to formulate power flow variables. At the same time, direct numerical integrations are also conducted to verify the analytical results. Power- and energy-based performance indices are introduced and used to evaluate the dynamic performance of the nonlinear absorber. At the end of this paper, conclusions and some suggestions for applications are provided.

2 Mathematical modelling

Figure 1 provides a schematic representation of a two degree-of-freedom (DOF) vibration absorption system, in which a vibrating primary structure, subject to a harmonic excitation with amplitude f and frequency ω, is modelled by a single DOF system consisting of a mass m_1, a nonlinear spring with restoring force $F(x_1)$ and a nonlinear damper with damping force $G_1(\dot{x}_1)$. To suppress its vibration, a light-weight mass m_2 is attached to the main structure through a nonlinear spring with restoring force $F_2(\delta)$ and a nonlinear viscous damper with damping force $G_2(\dot{\delta})$. It is assumed that the masses only have vertical displacement and their static equilibrium positions where the dynamic deflections $x_1 = x_2 = 0$ are taken as the reference. The relationships between the restoring and the damping forces and the corresponding dynamic deflections of the nonlinear springs and dampers are described by

$$G_1(\dot{x}_1) = c_{11}\dot{x}_1 + c_{12}\dot{x}_1^3, \tag{1a}$$

$$F_1(x_1) = k_{11}x_1 + k_{12}x_1^3, \tag{1b}$$

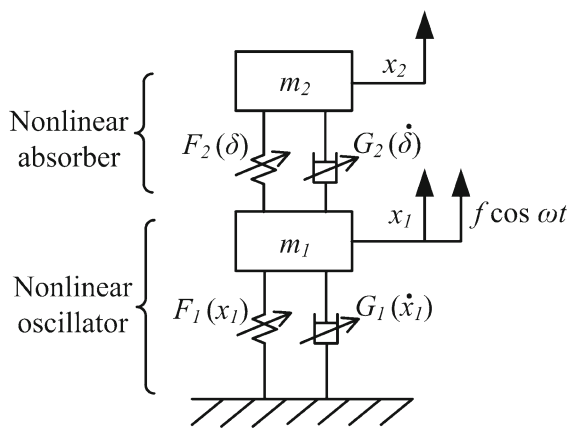

Fig. 1 A schematic model of the system

$$G_2(\dot{\delta}_1) = c_{21}\dot{\delta} + c_{22}\dot{\delta}^3, \tag{1c}$$
$$F_2(\delta) = k_{21}\delta_1 + k_{22}\delta_1^3, \tag{1d}$$

respectively, where $\delta = x_2 - x_1$ is the relative displacement of mass m_2 with respect to mass m_1, c_{11} and c_{21} are linear damping parameters, c_{12} and c_{22} are the nonlinear damping parameters, k_{11} and k_{21} are the linear stiffness parameters, k_{12} and k_{22} are nonlinear stiffness parameters of which zero, positive and negative values correspond to linear, hardening and softening springs, respectively.

The governing equations of motion of the system are obtained as

$$m_1\ddot{x}_1 + G_1(\dot{x}_1) + F_1(x_1) - G_2(\dot{\delta}_1) - F_2(\delta) = f\cos\omega t, \tag{2a}$$
$$m_2\ddot{x}_2 + G_2(\dot{\delta}_1) + F_2(\delta) = 0. \tag{2b}$$

To simplify these equations, the following non-dimensional parameters are introduced

$$x_0 = \frac{m_1 g}{k_{11}},\quad \mu = \frac{m_2}{m_1},\quad \omega_1 = \sqrt{\frac{k_{11}}{m_1}},\quad \omega_2 = \sqrt{\frac{k_{21}}{m_2}},$$
$$\gamma = \frac{\omega_2}{\omega_1},\quad \Omega = \frac{\omega}{\omega_1},\quad \xi_1 = \frac{c_{11}}{2m_1\omega_1},\quad \xi_2 = \frac{c_{21}}{2m_2\omega_2},$$
$$\eta = \frac{k_{12}}{k_{11}}x_0^2,\quad \epsilon = \frac{k_{22}}{k_{21}}x_0^2,\quad \lambda = \frac{c_{12}}{c_{11}}\omega_1^2 x_0^2,$$
$$\rho = \frac{c_{22}}{c_{21}}\omega_1^2 x_0^2,\quad f_0 = \frac{f}{k_{11}x_0},\quad y = \frac{\delta}{x_0},\quad x = \frac{x_1}{x_0},$$
$$\tau = \omega_1 t,$$

where x_0 is the reference displacement, μ is the mass ratio, ω_1 and ω_2 are the linearized natural frequency of the oscillator and that of the absorber, respectively, γ is the natural frequency ratio, and Ω is the non-dimensional excitation frequency, ξ_1 and ξ_2 are non-dimensional linear damping coefficients of the oscillator and the absorber, respectively, η and ϵ are the non-dimensional nonlinear stiffness coefficients of the oscillator and the absorber, respectively, λ and ρ are the non-dimensional nonlinear damping coefficients of the oscillator and the absorber, respectively, f_0 denotes non-dimensional forcing amplitude, y and x are non-dimensional displacement of the oscillator mass and the relative deflection of the absorber, respectively, τ is the non-dimensional time.

Following these definitions, the governing equations are written in a non-dimensional form

$$x'' + 2\xi_1 x'(1+\lambda x'^2) + x + \eta x^3 - \mu\gamma(2\xi_2 y'(1+\rho y'^2) + \gamma y + \epsilon\gamma y^3) = f_0\cos\Omega\tau, \tag{3a}$$
$$\mu y'' + \mu\gamma(2\xi_2 y'(1+\rho y'^2) + \gamma y + \epsilon\gamma y^3) = -\mu x'', \tag{3b}$$

where the primes denote differentiations with respect to the non-dimensional time τ.

To facilitate numerical and analytical investigations of power flow characteristics, equations (3a) and (3b) are transformed into a set of four first-order differential equations:

$$\begin{cases} x' = z \\ z' = f_0\cos\Omega\tau - 2\xi_1 z(1+\lambda z^2) - x - \eta x^3 \\ \qquad +\mu\gamma(2\xi_2 u(1+\rho u^2) + \gamma y + \epsilon\gamma y^3) \\ y' = u \\ u' = -f_0\cos\Omega\tau + 2\xi_1 z(1+\lambda z^2) + x + \eta x^3 \\ \qquad -\gamma(\mu+1)(2\xi_2 u(1+\rho u^2) + \gamma y + \epsilon\gamma y^3). \end{cases} \tag{4}$$

For performance assessment of nonlinear dynamic absorbers using vibrational power flow quantities, it is essential to solve Eq. (4) so that the influences of nonlinear parameters on the time-averaged power flow, as well as kinetic energies of the system can be obtained. However, when damping or stiffness nonlinearities exist, exact analytical solutions of the system response are not available. As an alternative, analytical approximations are sought in this paper, allowing evaluation of time-averaged power flow variables, as well as system kinetic energies at a relatively small computational cost. Direct numerical integrations based on the fourth-order Runge–Kutta method, although computationally more expensive, are also employed to reveal both transient and time-averaged power flow behaviours and to verify the analytical results.

3 Analytical approximations

The method of averaging [37] is used herein to derive a first-order approximation of the relationship between response amplitudes, phase angles and system parameters. For its implementation, the steady-state responses of the primary oscillator and the absorber are assumed

to be harmonic with the same frequency as the excitation, i.e.,

$$x = a\cos(\Omega\tau + \phi), \tag{5a}$$
$$x' = -a\Omega\sin(\Omega\tau + \phi), \tag{5b}$$
$$y = b\cos(\Omega\tau + \theta), \tag{5c}$$
$$y' = -b\Omega\sin(\Omega\tau + \theta), \tag{5d}$$

where a and b are the unknown response amplitudes, while ϕ and θ are the corresponding phase angles. Using the assumptions of the averaging method, Eq. (4) are transformed into

$$a'\cos(\Omega\tau + \phi) - a\phi'\sin(\Omega\tau + \phi) = 0, \tag{6a}$$
$$-a'\sin(\Omega\tau + \phi) - a\phi'\cos(\Omega\tau + \phi) = \frac{f_1}{\Omega}, \tag{6b}$$
$$b'\cos(\Omega\tau + \theta) - b\theta'\sin(\Omega\tau + \theta) = 0, \tag{6c}$$
$$-b'\sin(\Omega\tau + \theta) - b\theta'\cos(\Omega\tau + \theta) = \frac{f_2}{\Omega}, \tag{6d}$$

where

$$\begin{aligned} f_1 = {} & a\big(\Omega^2 - 1 - \eta a^2\cos^2(\Omega\tau + \phi)\big)\cos(\Omega\tau + \phi) \\ & + 2\xi_1 a\Omega\big(1 + \lambda a^2\Omega^2\sin^2(\Omega\tau + \phi)\big) \\ & \times \sin(\Omega\tau + \phi) + f_0\cos\Omega\tau + \mu\gamma f_3, \end{aligned} \tag{7a}$$
$$\begin{aligned} f_2 = {} & b\Omega^2\cos(\Omega\tau + \theta) + a'\Omega\sin(\Omega\tau + \phi) \\ & + (a\Omega^2 + a\Omega\phi')\cos(\Omega\tau + \phi) - \gamma f_3, \end{aligned} \tag{7b}$$
$$\begin{aligned} f_3 = {} & -2\xi_2 b\Omega\big(1 + \rho b^2\Omega^2\sin^2(\Omega\tau + \theta)\big) \\ & \times \sin(\Omega\tau + \theta) + \gamma b\big(1 + \epsilon b^2\cos^2(\Omega\tau + \theta)\big) \\ & \times \cos(\Omega\tau + \theta) \end{aligned} \tag{7c}$$

From Eqs. (6), the expressions of the time change rates of response amplitudes and phase angles are found

$$a' = -\frac{1}{\Omega}f_1\sin(\Omega\tau + \phi), \tag{8a}$$
$$\phi' = -\frac{1}{a\Omega}f_1\cos(\Omega\tau + \phi), \tag{8b}$$
$$b' = -\frac{1}{\Omega}f_2\sin(\Omega\tau + \theta), \tag{8c}$$
$$\theta' = -\frac{1}{b\Omega}f_2\cos(\Omega\tau + \theta). \tag{8d}$$

Assuming that the response amplitudes and the phase angles are slowing-varying variables of time, the left hand sides of Eqs. (8) can be approximated by their average values over an excitation cycle, i.e.,

$$a' \approx -\frac{1}{2\pi}\int_0^{\frac{2\pi}{\Omega}} f_1\sin(\Omega\tau + \phi)\,\mathrm{d}\tau, \tag{9a}$$
$$\phi' \approx -\frac{1}{2\pi a}\int_0^{\frac{2\pi}{\Omega}} f_1\cos(\Omega\tau + \phi)\,\mathrm{d}\tau, \tag{9b}$$
$$b' \approx -\frac{1}{2\pi}\int_0^{\frac{2\pi}{\Omega}} f_2\sin(\Omega\tau + \theta)\,\mathrm{d}\tau, \tag{9c}$$
$$\theta' \approx -\frac{1}{2\pi b}\int_0^{\frac{2\pi}{\Omega}} f_2\cos(\Omega\tau + \theta)\,\mathrm{d}\tau. \tag{9d}$$

Evaluating the integrations in Eq. (9) with reference to the previous expressions of f_1 and f_2, it follows that

$$\begin{aligned} a' = {} & -\frac{1}{\Omega}\Big(\frac{f_0}{2}\sin\phi + \xi_1 a\Omega\left(1 + \frac{3}{4}\lambda a^2\Omega^2\right) \\ & + \mu\gamma b\Big(-\xi_2\Omega\left(1 + \frac{3}{4}\rho b^2\Omega^2\right)\cos(\phi - \theta) \\ & + \frac{\gamma}{2}\left(1 + \frac{3}{4}\epsilon b^2\right)\sin(\phi - \theta)\Big)\Big), \end{aligned} \tag{10a}$$
$$\begin{aligned} \phi' = {} & -\frac{1}{a\Omega}\Big(\frac{f_0}{2}\cos\phi + \frac{1}{2}a\left(\Omega^2 - 1 - \frac{3}{4}\eta a^2\right) \\ & + \mu\gamma b\big(\xi_2\Omega\left(1 + \frac{3}{4}\rho b^2\Omega^2\right)\sin(\phi - \theta) \\ & + \frac{\gamma}{2}\left(1 + \frac{3}{4}\epsilon b^2\right)\cos(\phi - \theta)\big)\Big), \end{aligned} \tag{10b}$$
$$\begin{aligned} b' = {} & -\frac{1}{\Omega}\Big(\frac{a'\Omega}{2}\cos(\phi - \theta) - \frac{a\Omega^2 + a\Omega\phi'}{2} \\ & \times \sin(\phi - \theta) + \gamma\xi_2 b\Omega\left(1 + \frac{3}{4}\rho b^2\Omega^2\right)\Big), \end{aligned} \tag{10c}$$
$$\begin{aligned} \theta' = {} & -\frac{1}{b\Omega}\Big(\frac{b\Omega^2}{2} + \frac{a\Omega^2 + a\Omega\phi'}{2}\cos(\phi - \theta) \\ & + \frac{a'\Omega}{2}\sin(\phi - \theta) - \frac{\gamma^2 b}{2}\left(1 + \frac{3}{4}\epsilon b^2\right)\Big). \end{aligned} \tag{10d}$$

In the steady-state motion, the response amplitudes and phase angles remain unchanged, and thus their derivatives will vanish, i.e., $a' = \phi' = b' = \theta' = 0$. Based on this, Eq. (10) are simplified into

$$\begin{aligned} & \frac{f_0}{2}\sin\phi + \xi_1 a\Omega\left(1 + \frac{3}{4}\lambda a^2\Omega^2\right) \\ & + \mu\gamma b\Big(-\xi_2\Omega\left(1 + \frac{3}{4}\rho b^2\Omega^2\right)\cos(\phi - \theta) \end{aligned}$$

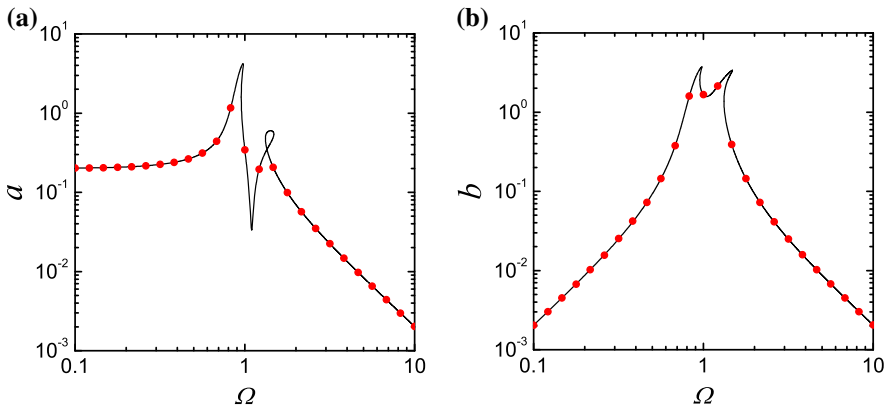

Fig. 2 Verification of the derived frequency-response relations ($\xi_1 = \xi_2 = 0.01$, $\eta = 0.01$, $\lambda = 0.1$, $\epsilon = 0.1$, $\rho = 0.1$, $\mu = 0.1$, $\gamma = 1.0$, $f_0 = 0.2$). *Lines* analytical approximations, dots: numerical integration results

$$+\frac{\gamma}{2}\left(1+\frac{3}{4}\epsilon b^2\right)\sin(\phi-\theta)\Big) = 0, \tag{11a}$$

$$\frac{f_0}{2}\cos\phi + \frac{1}{2}a(\Omega^2 - 1 - \frac{3}{4}\eta a^2) + \mu\gamma b\Big(\xi_2\Omega\left(1+\frac{3}{4}\rho b^2\Omega^2\right)\sin(\phi-\theta) + \frac{\gamma}{2}\left(1+\frac{3}{4}\epsilon b^2\right)\cos(\phi-\theta)\Big) = 0, \tag{11b}$$

$$-\frac{a\Omega^2}{2}\sin(\phi-\theta) + \gamma\xi_2 b\Omega\left(1+\frac{3}{4}\rho b^2\Omega^2\right) = 0, \tag{11c}$$

$$\frac{a\Omega^2}{2}\cos(\phi-\theta) + \frac{b\Omega^2}{2} - \frac{\gamma^2 b}{2}\left(1+\frac{3}{4}\epsilon b^2\right) = 0. \tag{11d}$$

Cancelling out the trigonometric terms with phase angles in Eqs. (11c) and (11d), we obtain

$$a^2\Omega^4 = (2\gamma\xi_2 b\Omega)^2\left(1+\frac{3}{4}\rho b^2\Omega^2\right)^2 + b^2\left(\gamma^2 - \Omega^2 + \frac{3}{4}\epsilon\gamma^2 b^2\right)^2. \tag{12}$$

Eliminating the terms with $\sin\phi$, $\cos\phi$, $\sin(\phi-\theta)$ or $\cos(\phi-\theta)$ in Eqs. (11a) and (11b) by Eqs. (11c) and (11d), we have

$$f_0^2 a^2 = 4\Omega^2\Big(\xi_1 a^2\left(1+\frac{3}{4}\lambda a^2\Omega^2\right) + \mu\gamma\xi_2 b^2\left(1+\frac{3}{4}\rho b^2\Omega^2\right)^2\Big)^2 + \left(a^2\left(\Omega^2 + \mu\Omega^2 - 1 - \frac{3}{4}\eta a^2\right) + \mu b^2\left(\gamma^2 + \frac{3}{4}\epsilon\gamma^2 b^2 - \Omega^2\right)\right)^2. \tag{13}$$

Thus, the relationship between the steady-state response amplitudes of the systems and different parameters is governed by Eqs. (12) and (13), which are nonlinear algebraic equations. Note that the unknown a^2 can be expressed in terms of b^2 and other parameters using Eq. (12). A substitution of the resultant expression to Eq. (13) to replace a^2 yields a nonlinear equation of b^2, which can be solved by a bisection algorithm [38]. The results provide first-order approximations of the response amplitudes. It can be observed that in these equations the nonlinear damping parameters λ and ρ and the nonlinear stiffness parameters ϵ and η always appear in the forms of $1 + \frac{3}{4}\lambda a^2\Omega^2$, $1 + \frac{3}{4}\rho b^2\Omega^2$, $1 + \frac{3}{4}\eta a^2$, and $1 + \frac{3}{4}\epsilon b^2$, respectively. In non-resonant regions, the values of $\frac{3}{4}\lambda a^2\Omega^2$, $\frac{3}{4}\rho b^2\Omega^2$, $\frac{3}{4}\eta a^2$ and $\frac{3}{4}\epsilon b^2$ may be much smaller than 1. Correspondingly, the effects of the nonlinear parameters on the response amplitudes a and b can be expected to be small as they may be neglected when solving Eqs. (12) and (13).

For a nonlinear system with parameters set as $\xi_1 = \xi_2 = 0.01$, $\eta = 0.01$, $\lambda = 0.1$, $\epsilon = 0.1$, $\rho = 0.1$, $\mu = 0.1$, $\gamma = 1.0$, $f_0 = 0.2$, Fig. 2 compares the fourth-order Runge-Kutta numerical integration results of the response amplitudes with those obtained using the averaging approximations. A good agreement of the results is shown, which verifies the averaging formulations. It shows some inherently nonlinear behaviour, i.e., the response amplitudes of the nonlinear system may become multi-valued at a single frequency and the peaks of the curves bent to the high frequencies. The corresponding power flow behaviour will be examined and shown in the following text.

As shown in Fig. 2, at some excitation frequencies, there may be more than one solution to Eqs. (12) and (13), i.e., non-unique steady-state responses may be

encountered. In this situation, it is useful to perform stability analysis of the solutions as only the stable ones are physically realisable and generally of more interest to engineering applications [37]. For clarity, Eqs. (10) are rewritten as

$$a' = u_1' = g_1(a, \phi, b, \theta), \tag{14a}$$

$$\phi' = u_2' = g_2(a, \phi, b, \theta), \tag{14b}$$

$$b' = u_3' = g_3(a, \phi, b, \theta), \tag{14c}$$

$$\theta' = u_4' = g_4(a, \phi, b, \theta), \tag{14d}$$

where the detailed expressions for $g_i (i = 1, 2, 3, 4)$ can be obtained from Eq. (10). The corresponding characteristic matrix of a solution $(a_s, \phi_s, b_s, \theta_s)$ to the frequency-response relations (12) and (13) is

$$A = \begin{pmatrix} a_{11} & a_{12} & a_{13} & a_{14} \\ a_{21} & a_{22} & a_{23} & a_{24} \\ a_{31} & a_{32} & a_{33} & a_{34} \\ a_{41} & a_{42} & a_{43} & a_{44} \end{pmatrix}, \tag{15}$$

where $a_{ij} = \frac{\partial g_i}{\partial u_j}, (i, j = 1, 2, 3, 4)$ of which the detailed expressions are omitted here. In the derivation, the property that for any solution point $(a_s, \phi_s, b_s, \theta_s)$, $g_i = 0 (i = 1, 2, 3, 4)$, may be used. The stability of a solution can then be identified by examining the corresponding eigenvalues of the matrix A. If the eigenvalues all have negative real part, the solution will be stable. On the other hand, if one of the eigenvalues of A is with a positive real part, the corresponding solution becomes unstable.

4 Power flow analysis

To assess the vibration absorption performance, the effects of the stiffness, as well as damping nonlinearities in the primary structure, as well as in the absorber on the vibration power generation, dissipation, transmission and absorption should be clarified. In the following content, power flow variables, as well as the maximum kinetic energies of the masses will be formulated analytically using the previously derived averaging results.

4.1 Input power

The non-dimensional instantaneous input power into the system is the product of the excitation with the corresponding velocity. In this system, there is only one excitation acting on mass m_1, so that we have

$$p_{in} = f_0 v_1 \cos \Omega \tau, \tag{16}$$

where v_1 is instantaneous velocity of the primary structure. When a first-order harmonic response is assumed, we have $v_1 = x' = -a\Omega \sin(\Omega\tau + \phi)$. Consequently, the time-averaged input power is formulated by

$$\bar{p}_{in}(\Omega) = \frac{1}{T} \int_0^T p_{in} \, \mathrm{d}\tau \approx -\frac{f_0 a \Omega}{2} \sin \phi, \tag{17}$$

where the averaging time T was taken as $\frac{2\pi}{\Omega}$, i.e., a cycle of the excitation. By replacing the trigonometric function $\sin\phi$ in (17) using the relations in Eq. (11) and further simplifying, the approximate expression of time-averaged input power (TAIP) is derived as

$$\bar{p}_{in}(\Omega) = \xi_1 a^2 \Omega^2 \left(1 + \frac{3}{4}\lambda a^2 \Omega^2\right) + \mu\gamma\xi_2 b^2 \Omega^2 \left(1 + \frac{3}{4}\rho b^2 \Omega^2\right). \tag{18}$$

4.2 Transmitted power

It is useful to clarify vibration energy transmission paths in the system. The power injected by the external excitation is partly transmitted downwards and dissipated by the nonlinear damper in the primary structure, while the rest is transmitted upwards through the nonlinear spring and nonlinear damper of the absorber to mass m_2. The instantaneous power transmitted to mass m_2 is the product of the force acting upon it with the corresponding velocity, i.e.,

$$p_t = f_t v_2, \tag{19}$$

where $f_t = \mu\gamma(2\xi_2 y' + \gamma y + \epsilon\gamma y^3)$ is the transmitted force and $v_2 = x' + y'$ is the velocity of mass m_2. The time-averaged transmitted power to mass m_2 over an excitation cycle is formulated by

$$\bar{p}_t(\Omega) = \frac{1}{T} \int_0^T p_t \, \mathrm{d}\tau. \tag{20}$$

Replacing the variables in the expressions of f_t and v_2 with their first-order analytical approximations and

completing the integration in Eq. (20), it follows that

$$\bar{p}_t(\Omega) = \mu\gamma\Big(\xi_2 b\Omega^2\big(a\cos(\phi-\theta)+b\big)\left(1+\frac{3}{4}\rho b^2\Omega^2\right) - \frac{\gamma ab\Omega}{2}\left(1+\frac{3}{4}\epsilon b^2\right)\sin(\phi-\theta)\Big). \tag{21}$$

Using the relationship described in Eq. (11) to eliminate the trigonometric functions in Eq. (21), it can be shown that

$$\bar{p}_t(\Omega) = 0. \tag{22}$$

This expression shows that there will be no net vibration energy transmission to mass m_2 over a period of motion. This is reasonable as the mass is considered as a rigid body with no internal damping so that over an oscillation cycle, the change in its kinetic energy will vanish. Consequently, the time-averaged transmitted power into mass m_2 will be zero.

4.3 Dissipated power

The dissipated power refers to the rate change of vibration energy that turned into heat by damping. For the system under investigation, the total instantaneous dissipated power is

$$p_d = f_{d1}x' + f_{d2}y', \tag{23}$$

where $f_{d1} = 2\xi_1 x'$ and $f_{d2} = 2\mu\gamma\xi_2 y'$ are the damping force of the damper in the absorber and that in the primary structure, respectively. The first term in Eq. (23) represents power dissipated by the primary structure, while the second denotes power dissipated by the absorber. The time-averaged dissipated power over an excitation cycle is

$$\bar{p}_d(\Omega) = \frac{1}{T}\int_0^T p_d\,\mathrm{d}\tau. \tag{24}$$

By replacing velocities x' and y' with their first-order expressions described by Eqs. (5b) and (5d), the instantaneous dissipated power can be expressed in a first-order form, using which to complete the integration in Eq. (24) leads to

$$\bar{p}_d(\Omega) = \xi_1 a^2\Omega^2\left(1+\frac{3}{4}\lambda a^2\Omega^2\right) + \mu\gamma\xi_2 b^2\Omega^2\left(1+\frac{3}{4}\rho b^2\Omega^2\right). \tag{25}$$

Comparing the Eq. (25) with Eq. (18), it can be clearly seen that the expressions for $\bar{p}_{in}$ and $\bar{p}_d$ are exactly the same. This is in accordance with the principle of power balance, i.e., over a cycle of oscillation, there will be no net changes in the kinetic and potential energies of the system, and the input energy by the external excitation is all dissipated by damping.

4.4 Absorbed power

The instantaneous power absorbed by the nonlinear absorber equals the power dissipated by its damper, and thus can be expressed by

$$p_a = f_{d2}y'. \tag{26}$$

The time-averaged absorbed power over a cycle of oscillation is

$$\bar{p}_a(\Omega) = \frac{1}{T}\int_0^T p_a\,\mathrm{d}\tau \approx \mu\gamma\xi_2 b^2\Omega^2\left(1+\frac{3}{4}\rho b^2\Omega^2\right). \tag{27}$$

where analytical approximations of f_{d2} and y' were used in the evaluation of the integration.

4.5 Kinetic energies

In the applications of vibration control devices, the squared values of velocity amplitudes or the kinetic energy of a structure are often used as cost functions to measure the control effectiveness [27]. For the current system in the steady-state motion, the non-dimensional maximum kinetic energy K_1 of mass m_1 is encountered when it has the maximum velocity

$$K_1 = \frac{1}{2}(|v_1|_{\max})^2 \approx \frac{1}{2}a^2\Omega^2, \tag{28}$$

where a first-order approximation of the velocity $v_1 = -a\Omega\sin(\Omega\tau+\phi)$ is used so that its amplitude $|v_1|_{max} = a\Omega$. Also, the non-dimensional mass of m_1 is used. Similarly, by Eqs. (5b) and (5d), the velocity of the nonlinear absorber mass m_2 is expressed as

$$v_2 = x' + y' = -a\Omega\sin(\Omega\tau+\phi) - b\Omega\sin(\Omega\tau+\theta), \tag{29}$$

with the its amplitude being

$$|v_2|_{\max} = \Omega\sqrt{(a^2+b^2)+2ab\cos(\phi-\theta)}. \tag{30}$$

Using Eq. (11d) to replace the cosine function in Eq. (30) and simplifying, the non-dimensional maximum kinetic energy of mass m_2 is found to be

$$K_2 = \frac{1}{2}\mu(|v_2|_{\max})^2 = \frac{1}{2}\mu(a^2-b^2)\Omega^2 + \mu\gamma^2 b^2\left(1+\frac{3}{4}\epsilon b^2\right). \tag{31}$$

where μ denotes the non-dimensional mass of the primary oscillator.

4.6 Vibration absorption performance

Here we introduce vibration power- and energy-based variables to assess the performance of nonlinear dynamic vibration absorbers. Note that for the nonlinear primary oscillator without adding the absorber, the frequency-response relation is obtained by setting $\mu = 0$ in Eq. (13):

$$f_0^2 = 4\xi_1^2 a_0^2\Omega^2\left(1+\frac{3}{4}\lambda a_0^2\Omega^2\right) + a_0^2\left(\Omega^2 - 1 - \frac{3}{4}\eta a^2\right) \tag{32}$$

where a_0 represents the response amplitude of the structure without attaching the absorber. Correspondingly, the time-averaged input power and the maximum kinetic energy are

$$\bar{p}_{in}(\Omega) \approx \xi_1 a^2\Omega^2\left(1+\frac{3}{4}\lambda a_0^2\Omega^2\right). \tag{33a}$$

$$K_{pri} \approx \frac{1}{2}a_0^2\Omega^2, \tag{33b}$$

respectively. The performance of the absorber may be assessed by comparing the kinetic energy of the primary structure with and without adding the absorber and also the amount of time-averaged input power before and after attaching the absorber.

In order to compare the vibration attenuation efficiency of nonlinear absorbers with that of their linear counterparts, power absorption ratio may be defined as the ratio of the amount of time-averaged absorbed power and the time-averaged input power, i.e.,

$$R_a = \frac{\mu\gamma\xi_2 b^2\Omega^2\left(1+\frac{3}{4}\rho b^2\Omega^2\right)}{\xi_1 a^2\Omega^2\left(1+\frac{3}{4}\lambda a^2\Omega^2\right)+\mu\gamma\xi_2 b^2\Omega^2\left(1+\frac{3}{4}\rho b^2\Omega^2\right)}. \tag{34}$$

Clearly, to enhance the performance of vibration absorbers, a large power absorption ratio is preferable.

5 Results and discussions

In this section, case studies are conducted to examine the performance of linear/nonlinear absorbers attached to linear/nonlinear primary oscillators. As stated previously, the response of the system is obtained from both analytical approximations using the averaging method and numerical integrations based on a fourth-order Runge-Kutta method. The non-dimensional values of power flow variables are obtained and are shown in the following figures in a decibel scale with a non-dimensional reference level of 10^{-12}. In the following figures, the lines denote analytical approximations, whereas the symbols represent numerical integration results. A relatively light absorber of mass ratio $\mu = 0.1$ is used in all the cases. Heavier absorber can be employed for enhancing vibration suppression performance, but in engineering design, there is usually a limit on the acceptable weight penalty which needs to be taken into consideration.

5.1 A nonlinear stiffness absorber attached to a linear oscillator ($\epsilon \neq 0$, $\rho = \eta = \lambda = 0$)

Here, vibration mitigation of a harmonically excited linear primary structure with $\eta = \lambda = 0$ using a nonlinear absorber with linear damping ($\rho = 0$), but nonlinear stiffness ($\epsilon \neq 0$) is considered. To examine the effects of the stiffness nonlinearity in the dynamic absorber on vibrational power flows, the nonlinear stiffness coefficient ϵ varies from -0.01, indicating a softening stiffness absorber, to 0.1, for a hardening stiffness absorber. The results for the linear absorber case of $\epsilon = 0$ are also provided for comparison. Other system parameters are set as $\xi_1 = \xi_2 = 0.01$, $\eta = \rho = \lambda = 0$, $\mu = 0.1$, $\gamma = 1.0$, $f_0 = 0.1$.

Figure 3 plots the variations of time-averaged input and absorbed powers with respect to the non-dimensional excitation frequency Ω. It shows that there is only one peak at around $\Omega = 1$ in the time-averaged input power curve for the primary oscillator without adding the absorber. When a linear absorber is attached, two peaks can be observed in each curve, and the amount of time-averaged input power at the original peak is greatly reduced. In comparison, if a nonlinear

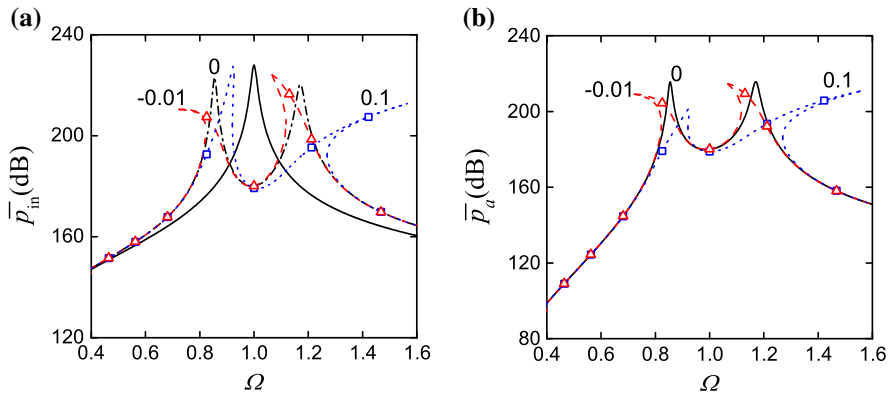

Fig. 3 Time-averaged **a** input and **b** absorbed powers of the system with a linear oscillator and an absorber with different nonlinear stiffness ($\xi_1 = \xi_2 = 0.01$, $\eta = \rho = \lambda = 0$, $\mu = 0.1$, $\gamma = 1.0$, $f_0 = 0.1$). *Solid line* without absorbers; *dashed line* or *triangles* $\epsilon = -0.01$; *dash-dotted line* $\epsilon = 0$; *dotted line* or *squares* $\epsilon = 0.1$

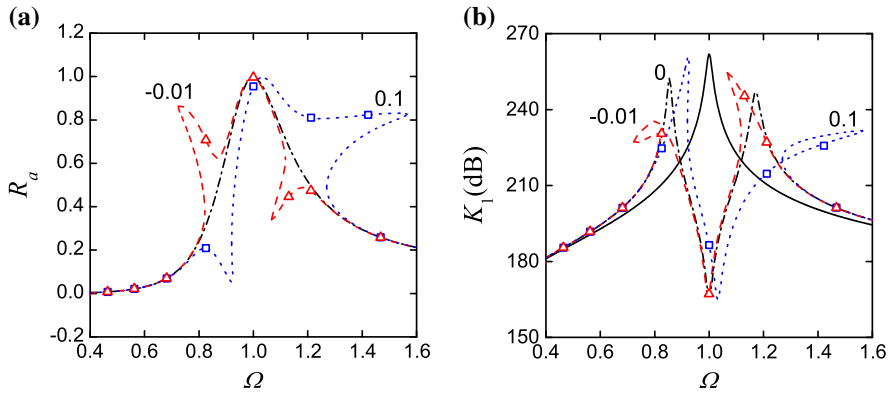

Fig. 4 Performance of the nonlinear stiffness absorber in vibration mitigation of a linear primary oscillator ($\xi_1 = \xi_2 = 0.01$, $\eta = \rho = \lambda = 0$, $\mu = 0.1$, $\gamma = 1.0$, $f_0 = 0.1$). **a** Power absorption ratio, and **b** kinetic energy of the oscillator. *Solid line* without absorbers; *dashed line* or *triangles* $\epsilon = -0.01$; *dash-dotted line* $\epsilon = 0$; *dotted line* or *squares* $\epsilon = 0.1$

stiffness absorber is used, there will still be two peaks in each curve, but they bend either to the high-frequency range when $\epsilon = 0.1$ or the low-frequency range when $\epsilon = -0.01$. Associated with the bending of the peaks, there are changes in the peak values of time-averaged power flows. For the softening absorber case of $\epsilon = -0.01$, the first peak of time-averaged input power $\bar{p}_{in}$ encountered in the low-frequency range becomes lower than that of corresponding linear absorber case, but the second peak value increases substantially. For the hardening absorber case of $\epsilon = 0.1$, the first peak value in $\bar{p}_{in}$ becomes larger than that of the corresponding linear system. However, the amount of time-averaged power flow reduces significantly around the second resonance peak of the linear absorber case. The twisting of curves also results in non-unique branches in some frequency ranges, indicating possible multiple solutions of power flows at a single excitation frequency. When the excitation frequency is away from the peak regions, the curves that correspond to different types of absorbers coincide with each other, and the time-averaged power flows are not sensitive to variations of ϵ. It indicates that the stiffness nonlinearity has local but not global effects on the power flow characteristics of the system.

The variations of the power absorption ratio and kinetic energy of the nonlinear oscillator are shown in Fig. 4a, b, respectively. The figures show that the examined linear and nonlinear absorbers are effective at around $\Omega = 1$ with a high power absorption ratio of $R_a \approx 1$ and a reduced kinetic energy compared with that of the primary oscillator without absorbers. However, the stiffness nonlinearities in the absorber affect the vibration absorption performance when Ω is close to the resonance frequencies of the integrated system. In the low-frequency range of $\Omega < 1$, a softening stiffness absorber performs well by increasing power absorption ratio and reducing peak kinetic energy. However, its performance in the high-frequency range of $\Omega > 1$ becomes worse than the linear absorber case, with a smaller R_a and a higher peak in kinetic energy K_1. In comparison, the hardening stiffness absorber with $\epsilon = 0.1$ enhances power absorption and attenuates the peak of kinetic energy in the high-frequency range of $\Omega > 1$. However, the correspond-

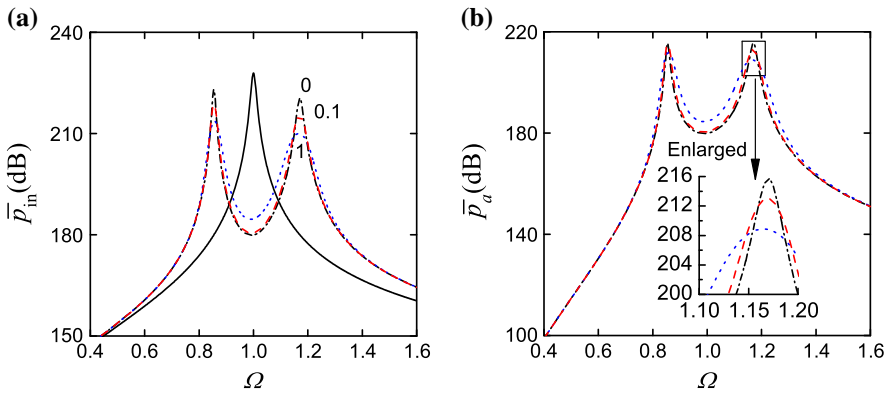

Fig. 5 Time-averaged **a** input and **b** absorbed powers of a system with a linear oscillator and an absorber with different nonlinear dampings ($\xi_1 = \xi_2 = 0.01, \epsilon = \eta = \lambda = 0, \mu = 0.1, \gamma = 1.0, f_0 = 0.1$). *Solid line* without absorbers; *dash-dotted line* $\rho = 0$; *dashed line* $\rho = 0.1$; *dotted line* $\rho = 1$

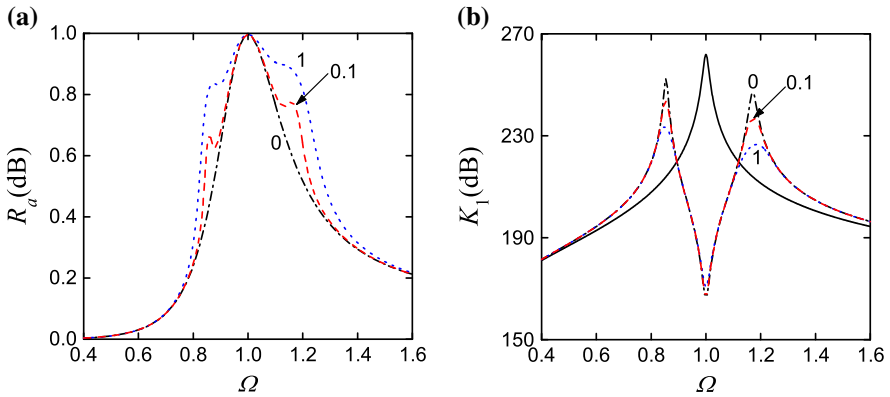

Fig. 6 Performance of the nonlinear damping absorber in vibration mitigation of a linear primary oscillator ($\xi_1 = \xi_2 = 0.01, \epsilon = \eta = \lambda = 0, \mu = 0.1, \gamma = 1.0, f_0 = 0.1$). **a** Power absorption ratio, and **b** kinetic energy of the primary structure. *Solid line* without absorbers; *dash-dotted line* $\rho = 0$; *dashed line* $\rho = 0.1$; *dotted line* $\rho = 1$

ing power absorption efficiency in the low-frequency range is compromised and the first peak of K_1 is larger than the corresponding linear absorber case.

In summary, for a linear primary structure, the results suggest that the softening (hardening) stiffness nonlinearity can be included in the absorber to enhance vibration mitigation in the low- (high-) frequency range as it can assist in: (1) reduction of the first (second) peak value of time-averaged power flow and the kinetic energy of the primary mass, (2) increase in power absorption ratio in the low- (high-) frequency range and (3) shift of the frequency band of effective vibration absorption to the lower (higher) frequencies.

5.2 A nonlinear damping absorber attached to a linear oscillator ($\rho \neq 0, \epsilon = \eta = \lambda = 0$)

To assess the performance of a vibration absorber with nonlinear damping in suppressing excessive vibrations of a linear primary oscillator, the system parameters are set as $\xi_1 = \xi_2 = 0.01, \epsilon = \eta = \lambda = 0, \mu = 0.1, \gamma = 1.0, f_0 = 0.1$, while the nonlinear damping parameter ρ of the absorber varies from 0 to 0.1 and then to 1. The time-averaged input power curves are depicted in Fig. 5, which shows that the peak time-averaged input and absorbed powers are reduced by having stronger nonlinear damping. However, between the resonant frequencies, a larger ρ gives rise to a slightly higher level of time-averaged power flows. In the other frequency ranges away from resonance, the time-averaged power flow variables are observed to be insensitive to the variations of ρ. The reason is that the corresponding response amplitude b of the absorber is small, so that the contribution of nonlinear damping $\frac{3}{4}\rho b^2\Omega^2$ in frequency-response relations (12) and (13) is small. The performance of nonlinear damping absorbers is examined in Fig. 6. It shows that a larger value of ρ leads to better power absorption around the resonance frequencies of the integrated system. Also, compared with the linear absorber case, the peaks in the kinetic energy of oscillator are reduced by increasing ρ.

To summarise, the cubic damping nonlinearity in the absorber can assist in reductions of peak time-averaged

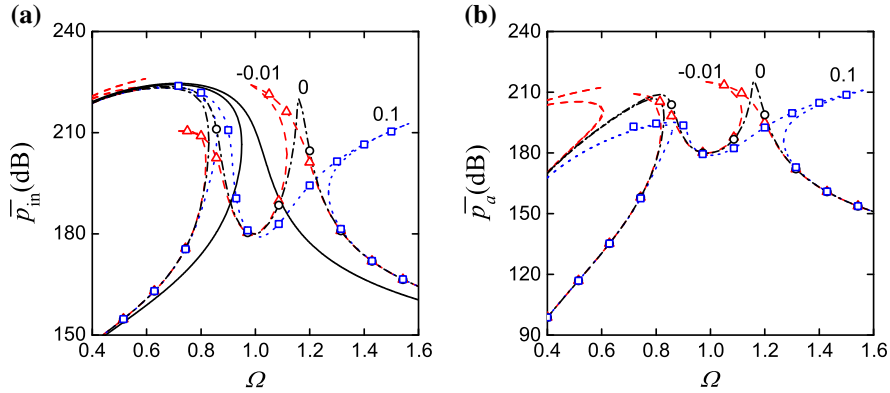

Fig. 7 Time-averaged **a** input and **b** absorbed powers of a system with a softening stiffness oscillator and an absorber with different nonlinear stiffnesses ($\xi_1 = \xi_2 = 0.01, \mu = 0.1, \gamma = 1, f_0 = 0.1, \eta = -0.02, \rho = \lambda = 0$). *Solid line* without absorbers; *dash-dotted line* or *circles* $\epsilon = 0$; dashed line or *triangles* $\epsilon = -0.01$; *dotted line* or *squares* $\epsilon = 0.1$

power flow levels. The resonance peaks of the kinetic energy of the primary structure are also suppressed. At the same time, the power absorption ratio becomes larger than the corresponding linear case. These characteristics suggest that the cubic damping nonlinearity in the absorber can be introduced to improve the performance of vibration absorbers.

5.3 Nonlinear absorbers attached to a softening oscillator ($\eta < 0, \epsilon \neq 0$)

The previous cases considered the existence of stiffness or damping nonlinearity in the absorber. However, in some applications significant nonlinearity exists in the primary oscillator as well. In this situation, absorbers that are designed under the assumption of the primary structure being linear may not be effective. It is thus necessary to examine the effectiveness of nonlinear absorbers for different types of nonlinear oscillators. The outcome of such investigations can provide guidance for a proper design of the absorber's nonlinearity with respect to the existing nonlinear characteristics of the primary structure. For clarity, this section considers a softening stiffness primary oscillator attached with different nonlinear absorbers, while the next section will focus on suppressing the vibrations of a hardening stiffness primary oscillator using nonlinear absorbers.

Figure 7 shows the variations of time-averaged power flow variables for a system with $\xi_1 = \xi_2 = 0.01, \mu = 0.1, \gamma = 1, f_0 = 0.1, \eta = -0.02, \rho = \lambda = 0$. The primary oscillator is of softening stiffness, while the absorber possesses softening stiffness when $\epsilon = -0.01$ or hardening stiffness when $\epsilon = 0.1$. The results for a linear absorber case with $\epsilon = 0$ are also provided in the figure for comparison. The figure shows that the time-averaged input power curve of the nonlinear oscillator without adding an absorber bends to the low-frequency range. Compared with that, attaching the softening stiffness absorber of $\epsilon = -0.01$ to the softening stiffness primary structure strengthens the overall softening nonlinearity of the system, as demonstrated by the further twisting of the peaks to the low-frequency range. It also results in multiple solutions of power flow variables over a larger range of excitation frequencies, including the original tuning frequency $\Omega = 1$ of a linear absorber. In contrast, adding a hardening stiffness absorber of $\epsilon = 0.1$ to the softening oscillator bends, the second peak in the power flow curves to the high-frequency range, while keeping the first peak extended to the low-frequency range. The original second peak in time-averaged input power of the linear absorber case is effectively suppressed.

Figure 8 examines the performance of the absorbers by evaluating the corresponding power absorption ratio and the kinetic energy of the primary oscillator. It shows that although introducing a softening stiffness characteristic in the absorber can increase power absorption ratio R_a in the low-frequency range, at higher excitation frequencies with Ω locating approximately in between 0.98 and 1.2, the value of R_a may become smaller than that of the corresponding linear absorber

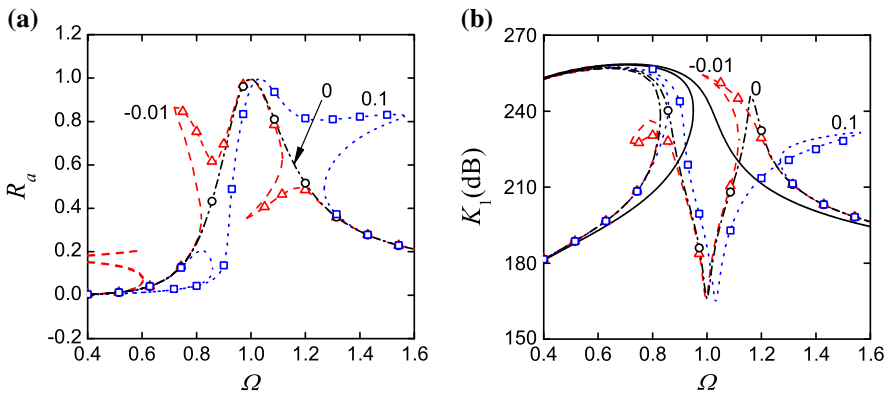

Fig. 8 Performance of nonlinear stiffness absorbers in vibration mitigation of a softening stiffness oscillator ($\xi_1 = \xi_2 = 0.01$, $\mu = 0.1$, $\gamma = 1$, $f_0 = 0.1$, $\eta = -0.02$, $\rho = \lambda = 0$). **a** Power absorption ratio and **b** kinetic energy of the primary structure. *Solid line* without absorbers; *dash-dotted line* or *circles* $\epsilon = 0$; *dashed line* or *triangles* $\epsilon = -0.01$; *dotted line* or *squares* $\epsilon = 0.1$

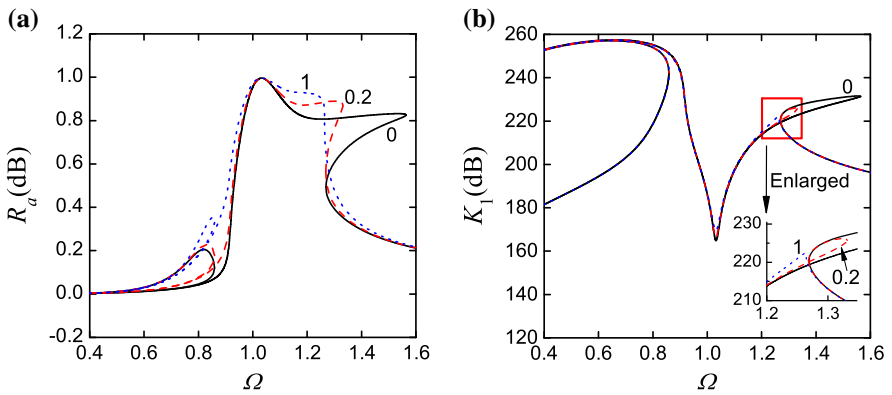

Fig. 9 Performance of absorbers with combined damping and stiffness nonlinearities in vibration mitigation of a softening stiffness oscillator ($\xi_1 = \xi_2 = 0.01$, $\mu = 0.1$, $\gamma = 1$, $f_0 = 0.1$, $\eta = -0.02$, $\epsilon = 0.1$, $\lambda = 0$). **a** Power absorption ratio, and **b** kinetic energy of the primary oscillator. *Solid line* $\rho = 0$; *dashed line* $\rho = 0.2$; *dotted line* $\rho = 1$

case. Also in this frequency range, the kinetic energy of the primary structure attached with the softening absorber may be much larger than that of the structure without using the absorber. At $\Omega = 1$, R_a and K_1 become multiple-valued and sensitive to the initial conditions. These characteristics are not desirable for effective vibration absorption. When a hardening stiffness absorber with $\epsilon = 0.1$ is used, the kinetic energy of the nonlinear oscillator remains single-valued over a wider range of excitation frequencies with Ω approximately in between 0.86 and 1.26. Clearly, it provides better vibration absorption performance than the corresponding linear absorber when $1.03 < \Omega < 1.25$, as the value of R_a is larger. At the same time the second peak of K_1 of is greatly suppressed, compared with the linear absorber case. Clearly, a hardening stiffness absorber can be added to a softening nonlinear structure to effectively mitigate its vibrations.

In Fig. 9, the influences of adding damping nonlinearity to the hardening absorber on its performance are investigated. The primary oscillator is still of softening stiffness. The system parameters are set as $\xi_1 = \xi_2 = 0.01$, $\mu = 0.1$, $\gamma = 1$, $f_0 = 0.1$, $\eta = -0.02$, $\epsilon = 0.1$, $\lambda = 0$, while the nonlinear damping parameter ρ varies from 0 to 0.2, and then to 1. Figure 9a shows that by increasing ρ, there is a narrower range of multiple solution branches of power flows at high excitation frequencies of $\Omega > 1$. It is also observed that R_a increases with ρ when the excitation frequency Ω locates approximately between 1.1 and 1.28. Compared with the case with linear damping $\rho = 0$, the second peak value of K_1 is substantially suppressed when stronger nonlinear damping is introduced to the absorber. It should also be noted that when excitation frequency Ω is away from the second resonance peak, the kinetic energy of the primary oscillator is shown not sensitive to the changes in ρ.

In summary, when the primary structure is of softening stiffness nonlinearity, addition of a softening stiffness absorber may not provide desirable performance as it will result in a stronger softening nonlinearity in the overall system. Consequently, the resonant peaks will be bent further to the low-frequency range. Around the tuning frequency, the absorption performance may be compromised with non-unique solutions, potentially high level of power flow and

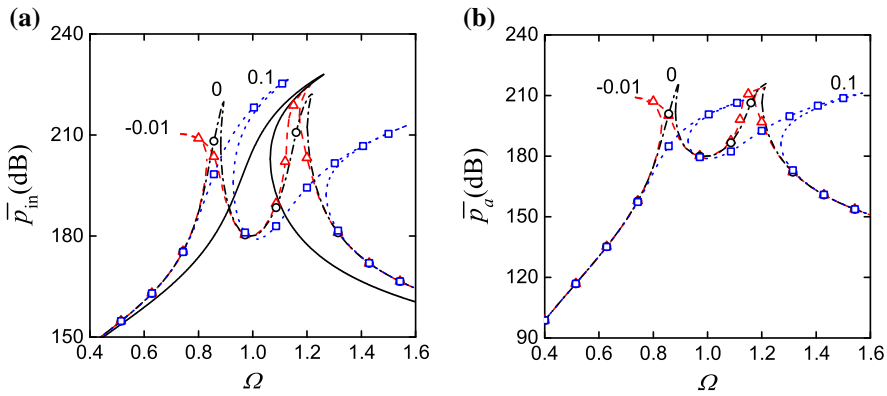

Fig. 10 Time-averaged **a** input and **b** absorbed powers of a system with a hardening stiffness oscillator, and an absorber with different nonlinear stiffnesses ($\xi_1 = \xi_2 = 0.01, \mu = 0.1, \gamma = 1, f_0 = 0.1, \eta = 0.05, \lambda = \rho = 0$). *Solid line* without absorbers; *dash-dotted line* or *circles* $\epsilon = 0$; *dashed line* or *triangles* $\epsilon = -0.01$; *dotted line* or *squares* $\epsilon = 0.1$

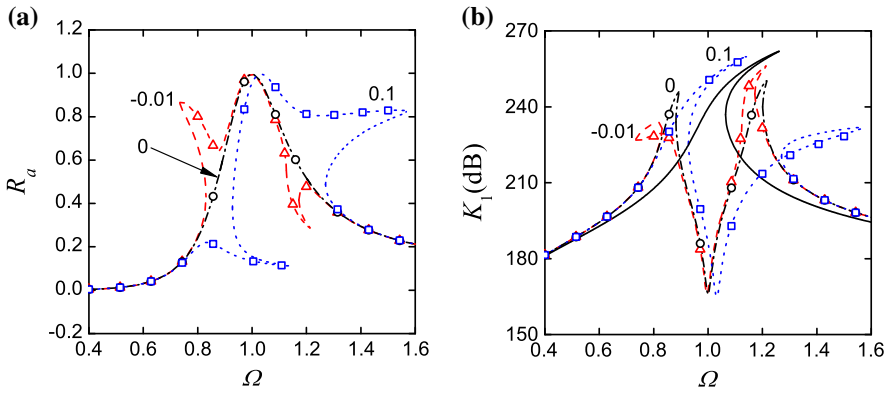

Fig. 11 Performance of nonlinear stiffness absorbers in vibration mitigation of a hardening stiffness oscillator ($\xi_1 = \xi_2 = 0.01, \mu = 0.1, \gamma = 1, f_0 = 0.1, \eta = 0.05, \lambda = \rho = 0$). **a** Power absorption ratio, and **b** kinetic energy of the primary oscillator. *Solid line* without absorbers; *dash-dotted line* or *circles* $\epsilon = 0$; *dashed line* or *triangles* $\epsilon = -0.01$; *dotted line* or *squares* $\epsilon = 0.1$

large kinetic energy. In comparison, introduction of a hardening stiffness absorber can bend the second peak to the higher-frequency range, creating a larger frequency band of effective vibration mitigation. Therefore, hardening stiffness can be used in the absorber for enhanced vibration absorption from a softening primary structure.

5.4 Nonlinear absorbers attached to a hardening oscillator ($\eta > 0, \epsilon \neq 0$)

In this section, the performance of different types of nonlinearities in the absorbers in vibration suppression of a oscillator with hardening stiffness is investigated. For a system with $\xi_1 = \xi_2 = 0.01, \mu = 0.1, \gamma = 1, f_0 = 0.1, \eta = 0.05, \lambda = \rho = 0$, the nonlinear stiffness parameter ϵ of the absorber is set as -0.01 for a softening stiffness absorber and 0.1 for a hardening stiffness absorber. To compare the performance of linear and nonlinear absorbers, the results for the system with a linear absorber with $\epsilon = 0$ attached to the hardening stiffness oscillator are also plotted in the figures.

Figure 10 shows that for the primary oscillator without attaching absorbers, the resonant peak in time-averaged input power curve extends to the high-frequency range. When a linear absorber with $\epsilon = 0$ is attached to the main oscillator, two peaks can be identified in the time-averaged input power curve and they both bend slightly towards the high frequencies. Compare with that, an introduction of the hardening stiffness absorber with $\epsilon = 0.1$ to the nonlinear oscillator yields further bending of the peaks to the higher frequencies. The figures show non-unique time-averaged power flow levels at some excitation frequencies, including the tuning frequency $\Omega = 1$ of the corresponding linear absorber. This may not be wanted for vibration absorption as the performance of the absorber will be dependent on the initial conditions. In contrast, the use of the softening stiffness absorber with $\epsilon = -0.01$ to the hardening oscillator, however, results in the twisting of the first peak towards the low-frequency range and the second peak to the high frequencies. At the same time, the time-averaged power flow variables remain small and single-valued in a relatively wider frequency range

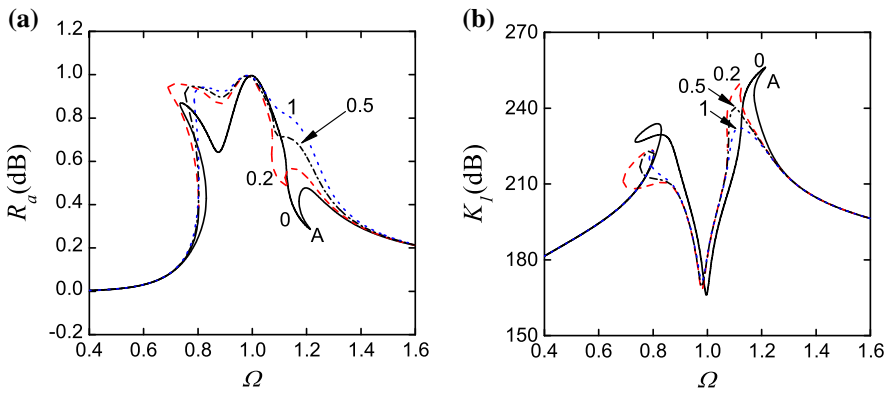

Fig. 12 Performance of absorbers with combined damping and stiffness nonlinearities in vibration mitigation of a hardening stiffness oscillator ($\xi_1 = \xi_2 = 0.01, \mu = 0.1, \gamma = 1, f_0 = 0.1, \eta = 0.05, \epsilon = -0.01, \lambda = 0$). **a** Power absorption ratio, and **b** kinetic energy of the primary oscillator. *Solid line* $\rho = 0$; *dashed line* $\rho = 0.2$; *dash-dotted line* $\rho = 0.5$; *dotted line* $\rho = 1$

around the tuning frequency of $\Omega = 1$. This behaviour may be employed for effective vibration absorption.

Figure 11 compares the power absorption ratio, as well as the kinetic energy of the nonlinear oscillator when the absorber is of different stiffness characteristics. The figure shows that the considered softening stiffness absorber performs well in the low-frequency range where the excitation frequency $\Omega < 1$, as the corresponding power absorption ratio R_a is increased. Moreover, the kinetic energy K_1 remains single-valued around $\Omega = 1$ with first peak lower than that of the case with a linear absorber. These characteristics clearly show the benefits of using the softening stiffness absorber for low-frequency vibration absorption. When $\Omega > 1$, it is observed that adding the hardening absorber successfully improves power absorption efficiency with R_a becoming larger. Also, the second peak value of K_1 is greatly reduced from the linear absorber case. However, when the hardening stiffness absorber is used, there are non-unique and small values of power absorption ratio R_a when Ω is close to one. At the same time, the kinetic energy K_1 is also multiple-valued and potentially large. As a result, hardening stiffness in the absorber may not be desirable for vibration suppression of the hardening oscillator around its linearized natural frequency $\Omega = 1$.

Figure 12 investigates the effects of nonlinear damping on the performance of the softening stiffness absorber attached to a hardening oscillator. The nonlinear damping parameter ρ of the absorber changes from 0, to 0.2, 0.5 and then to 1, and the other system parameters are set as $\xi_1 = \xi_2 = 0.01, \mu = 0.1, \lambda = 1, f_0 = 0.1, \eta = 0.05, \epsilon = -0.01, \lambda = 0$. It shows that the power absorption ratio R_a increases with ρ when Ω locates approximately between 0.8 and 1. As the nonlinear damping becomes stronger, the value of R_a is enlarged at higher excitation frequencies around $\Omega = 1.2$. For the influence of parameter ρ on the kinetic energy of the nonlinear oscillator, Fig. 12(b) shows that both peaks in kinetic energy curve are suppressed by increasing the nonlinear damping in the absorber. Also, the frequency ranges of multiple solutions become much narrower. Again, the results indicate possible benefits of introducing the nonlinear damping in the absorber for better performance.

To summarise, when the primary structure is of hardening stiffness, an addition of a hardening stiffness absorber leads to a stronger hardening stiffness nonlinearity in the integrated system. As a result, there is a greater bending of resonance peaks in both time-averaged power flow and kinetic energy to the high-frequency range. Successful vibration mitigation at the original tuning frequency may not be guaranteed due to possible non-unique solutions. In comparison, the application of a softening stiffness absorber can widen the frequency range of effective absorption by bending the first resonant peak to the low frequencies and the second to the high frequencies. The kinetic energy of the oscillator remains low and single-valued in a larger frequency band. Thus, softening stiffness nonlinearity can be used for vibration attenuation of a hardening stiffness primary structure.

6 Conclusions

The paper investigated a two-degree-of-freedom system to evaluate the dynamic performance of nonlinear absorbers attached to a nonlinear primary oscillator from a vibrational power flow viewpoint. Power absorption ratio and the kinetic energy of the nonlinear

oscillator were used as performance indices. Different combinations of cubic damping and stiffness nonlinearities in the oscillator and absorber were investigated. Based on the investigations, the following conclusions and suggestions for nonlinear absorber design may be provided:

1. For a linear primary oscillator, attaching a softening (hardening) stiffness absorber can enhance power absorption and reduce kinetic energy when the excitation frequency is in the vicinity of the first (second) resonance at low frequency. In this way, the effective working frequency range of the absorber is shifted slightly to the lower (higher) frequencies.
2. Attaching a nonlinear damping absorber to a linear primary oscillator can help suppress peak values of time-averaged power flows and kinetic energy of the oscillator, and to enhance power absorption.
3. When the oscillator and absorber are both with hardening (softening) stiffness, the overall hardening (softening) nonlinearity of the system becomes greater. As a result, the resonant peaks in time-averaged power flow and kinetic energy curves will tend to bend more towards the high- (low-) frequency range. This may worsen the effectiveness of the absorber as the primary oscillator may experience non-unique and potentially high levels of kinetic energy at the desired functioning frequencies of the absorber.
4. A hardening stiffness absorber can be attached to a softening primary oscillator so as to effectively mitigation vibration in a wide frequency range, where the power absorption ratio is large and the kinetic energy remains low and single-valued.
5. When the oscillator is of hardening stiffness, a softening stiffness absorber can provide better performance than its hardening stiffness counterpart around the tuning frequency as it yields better vibration suppression by enhancing power absorption and reducing kinetic energy of the oscillator.
6. When nonlinear stiffness absorbers are used for nonlinear primary oscillators, adding cubic damping in the absorber can improve power absorption at the resonance peaks, and reduce the peak kinetic energies. Thus, the cubic damping nonlinearity is beneficial for vibration absorption as the frequency band of effective vibration attenuation is enlarged.

It should also be noted that the derived analytical formulations of the frequency-response relations allow more detailed parametric studies. It is also possible to conduct optimal design analysis of the absorber to determine optimal mass or damping ratios, and nonlinear stiffness and damping coefficients so as to achieve specific objectives, e.g., to suppress peak responses or to enlarge working frequency band. Moreover, the analytical/numerical analysis approach developed in the paper can easily be extended to deal with other types of nonlinearities in the absorber and the oscillator, with damping and restoring forces represented by polynomial or trigonometric functions of velocity and dynamic deflection, respectively.

References

1. Frahm, H.: A device for damping vibrations of bodies. US Patent, 989958 (1911)
2. Ormondroyd, J., Den Hartog, J.P.: The theory of the dynamic vibration absorber. J. Appl. Mech. **50**, 9–22 (1928)
3. Den Hartog, J.P.: Mechanical Vibrations, 4th edn. McGraw-Hill, New York (1956)
4. Snowdon, J.C.: Vibration of simply supported rectangular and square plates to which lumped masses and dynamic vibration absorbers are attached. J. Acoust. Soc. Am. **57**, 646–654 (1975)
5. Ozer, M.B., Rosyton, T.J.: Extending Den Hartog's vibrations absorber technique to multi-degree-of-freedom systems. J. Vib. Acoust. **127**, 1307–1320 (2005)
6. Roberson, R.E.: Synthesis of a nonlinear dynamic vibration absorber. J. Frankl. Inst. **254**, 205220 (1952)
7. Pipes, L.A.: Analysis of a non-linear vibration absorber. J. Appl. Mech. **20**, 515–518 (1953)
8. Arnold, F.R.: Steady state behaviour of systems provided with non-linear dynamic vibration absorbers. J. Appl. Mech. **22**, 487–492 (1955)
9. Hunt, J.B., Nissen, J.-C.: The broadband dynamic vibration absorber. J. Sound Vib. **83**, 573–578 (1982)
10. Rice, H.J.: Combinational instability of the non-linear vibration absorber. J. Sound Vib. **108**, 526–532 (1986)
11. Jordanov, I.N., Cheshankov, B.I.: Optimal design of linear and non-linear dynamic vibration absorbers. J. Sound Vib. **123**, 157–170 (1988)
12. Lazer, A.C., McKenna, P.J.: Large-amplitude periodic oscillations in suspension bridges: some new connections with nonlinear analysis. SIAM Rev. **32**, 537–578 (1990)
13. Kim, G., Singh, R.: A study of passive and adaptive hydraulic engine mount systems with emphasis on nonlinear characteristics. J. Sound Vib. **179**, 427–453 (1995)
14. Natsiavas, S.: Steady state oscillations and stability of nonlinear dynamic vibration absorbers. J. Sound Vib. **156**, 227–245 (1992)
15. Bonsel, J.H., Fey, R.H.B., Nijimeijer, H.: Applications of a dynamic vibration absorber to a piecewise linear beam system. Nonlinear Dyn. **37**, 227–243 (2004)
16. Jo, H., Yabuno, H.: Amplitude reduction of primary resonance of nonlinear oscillator by a dynamic vibration absorber using nonlinear coupling. Nonlinear Dyn. **55**, 67–78 (2009)

17. Viguié, R., Kerschen, G.: Nonlinear vibration absorber coupled to a nonlinear primary system: a tuning methodology. J. Sound Vib. **326**, 780–793 (2009)
18. Ji, J.C., Zhang, N.: Suppression of the primary resonance vibrations of a forced nonlinear systems using a dynamic vibration absorber. J. Sound Vib. **329**, 2044–2056 (2010)
19. Oueini, S.S., Nayfeh, A.H., Pratt, J.R.: A nonlinear vibration absorber for flexible structures. Nonlinear Dyn. **15**, 259–282 (1998)
20. Febbo, M., Machado, S.P.: Nonlinear dynamic vibration absorbers with saturation. J. Sound Vib. **332**, 1465–1483 (2013)
21. Goyder, H.G.D., White, R.G.: Vibrational power flow from machines into built-up structures. J. Sound Vib. **68**, 59–117 (1980)
22. Pinnington, R.J., White, R.G.: Power flow through machine isolators to resonant and non-resonant beams. J. Sound Vib. **75**, 179–197 (1992)
23. Xing, J.T., Price, W.G.: A power-flow analysis based on continuum dynamics. Philos. Trans. R. Soc. Lond. A **455**, 401–436 (1999)
24. Mace, B.R., Shorter, P.J.: Energy flow models from finite element analysis. J. Sound Vib. **233**, 369–389 (2000)
25. Xiong, Y.P., Xing, J.T., Price, W.G.: Power flow analysis of complex coupled systems by progressive approaches. J. Sound Vib. **239**, 275–295 (2001)
26. Xiong, Y.P., Xing, J.T., Price, W.G.: A general linear mathematical model of power flow analysis and control for integrated structure-control systems. J. Sound Vib. **267**, 301–334 (2003)
27. Xiong, Y.P., Xing, J.T., Price, W.G.: A power flow mode theory based on a system's damping distribution and power flow design approaches. Philos. Trans. R. Soc. Lond. A **461**, 3381–3411 (2005)
28. Zilletti, M., Elliott, S.J., Rustighi, E.: Optimisation of dynamic vibration absorbers to minimise kinetic energy and maximise internal power dissipation. J. Sound Vib. **331**, 4093–4100 (2012)
29. Royston, T.J., Singh, R.: Vibratory power flow through a nonlinear path into a resonant receiver. J. Acoust. Soc. Am. **101**, 2059–2069 (1997)
30. Xing, J.T., Price, W.G.: A substructure method for power flow analysis of non-linear systems consisting of linear substructures and non-linear controllers. Proceedings of the Eleventh International Congress on Sound and Vibration, St. Petersburg. pp. 2657–2664 (2004)
31. Xiong, Y.P., Xing, J.T., Price, W.G.: Interactive power flow characteristics of an integrated equipment-nonlinear isolator-travelling flexible ship excited by sea waves. J. Sound Vib. **287**, 245–276 (2005)
32. Vakakis, A.F., Gendelman, O.V., Bergman, L.A., McFarland, D.M., Kerschen, G., Lee, Y.S.: Nonlinear Targeted Energy Transfer in Mechanical and Structural Systems. Springer, New York (2008)
33. Xiong, Y., Cao, Q.: Power flow characteristics of coupled linear and nonlinear oscillators with irrational nonlinear stiffness. Proceedings of the Seventh European Nonlinear Dynamics Conference (ENOC), Rome, CDROM (2011)
34. Yang, J.: Power Flow Analysis of Nonlinear Dynamical Systems, PhD thesis, University of Southampton, Southampton (2013)
35. Yang, J., Xiong, Y.P., Xing, J.T.: Dynamics and power flow behaviour of a nonlinear vibration isolation system with a negative stiffness mechanism. J. Sound Vib. **332**, 167–183 (2013)
36. Yang, J., Xiong, Y.P., Xing, J.T.: Nonlinear power flow analysis of the Duffing oscillator. Mech. Syst. Signal Process. **45**, 563–578 (2014)
37. Nayfeh, A.H., Mook, D.T.: Nonlinear Oscillations. Willey, New York (1979)
38. Press, W.H., Flannery, B.P., Teukolsky, S.A., Vetterling, W.T.: Numerical Recipes: The Art of Scientific Computing. Cambridge University Press, Cambridge (1986)